Contraction behaviors of *Vorticella* sp. stalk investigated using high-speed video camera. II: Viscosity effect of several types of polymer additives

Junko Kamiguri[1], Noriko Tsuchiya[1], Ruri Hidema[1], Zenji Yatabe[1], Masahiko Shoji[2], Chihiro Hashimoto[3], Robert Bernard Pansu[4] and Hideharu Ushiki[5]

[1]*United Graduate School of Agricultural Science, Tokyo University of Agriculture and Technology, 3-5-8 Saiwai-cho, Fuchu-shi, Tokyo 183-8509, Japan*
[2]*Department of Applied Physics, Tokyo University of Agriculture and Technology, 2-24-16 Nakamachi Koganei-shi, Tokyo 184-8588, Japan*
[3]*Department of Applied Chemistry and Biotechnology, Niihama National College of Technology, 7-1 Yakumo-Cho, Niihama, Ehime 792-8580, Japan*
[4]*Laboratoire de Photophysique et Photochimie Supramoléculaires et Macromoléculaires, UMR 8531 CNRS, D'Alembert Institute, ENS Cachan, 61 av. President Wilson, F-94230 Cachan, France*
[5]*Institute of Agriculture, Tokyo University of Agriculture and Technology, 3-5-8 Saiwai-cho, Fuchu-shi, Tokyo 183-8509, Japan*

The contraction process of living *Vorticella* sp. in polymer solutions with various viscosities has been investigated by image processing using a high-speed video camera. The viscosity of the external fluid ranges from 1 to 5 mPa·s for different polymer additives such as hydroxypropyl cellulose, polyethylene oxide, and Ficoll. The temporal change in the contraction length of *Vorticella* sp. in various macromolecular solutions is fitted well by a stretched exponential function based on the nucleation and growth model. The maximum speed of the contractile process monotonically decreases with an increase in the external viscosity, in accordance with power law behavior. The index values approximate to 0.5 and this suggests that the viscous energy dissipated by the contraction of *Vorticella* sp. is constant in a macromolecular environment.

Corresponding author: Chihiro Hashimoto, Department of Applied Chemistry and Biotechnology, Niihama National College of Technology, 7-1 Yakumo-Cho, Niihama, Ehime 792-8580, Japan.
e-mail: hashimoto@chem.niihama-nct.ac.jp

Vorticella sp. is a stalked protozoan that is one of the fastest cellular machines in various systems to generate cellular- and molecular-level movement[1]. It consists of a slender stalk (100–500 μm in length and 2–3 μm in diameter) and a bell-shaped zooid (30–60 μm in diameter). The stalk is attached to a substrate, and it contracts spontaneously within milliseconds and re-extends in a few seconds[2–9]. The spasmoneme, the organelle placed helically in the stalk, is responsible for the contraction of the stalk, as shown in Figure 1. The spasmoneme (1–2 μm in diameter) consists of bundles of filaments (2–3 nm in diameter) and shrinks along the longitudinal direction. The spasmoneme of glycerinated *Vorticella* sp. contracts when Ca^{2+} is added and re-extends when Ca^{2+} is removed using a calcium agent such as EDTA and EGTA[2–6]. It is noted that Ca^{2+} induces the contraction of spasmoneme and that the hydrolysis of ATP is not necessary for the contraction[5]. The mechanism of contraction is still not clear at the molecular level; however, the contractility of the spasmoneme without the hydrolysis of ATP is funda-
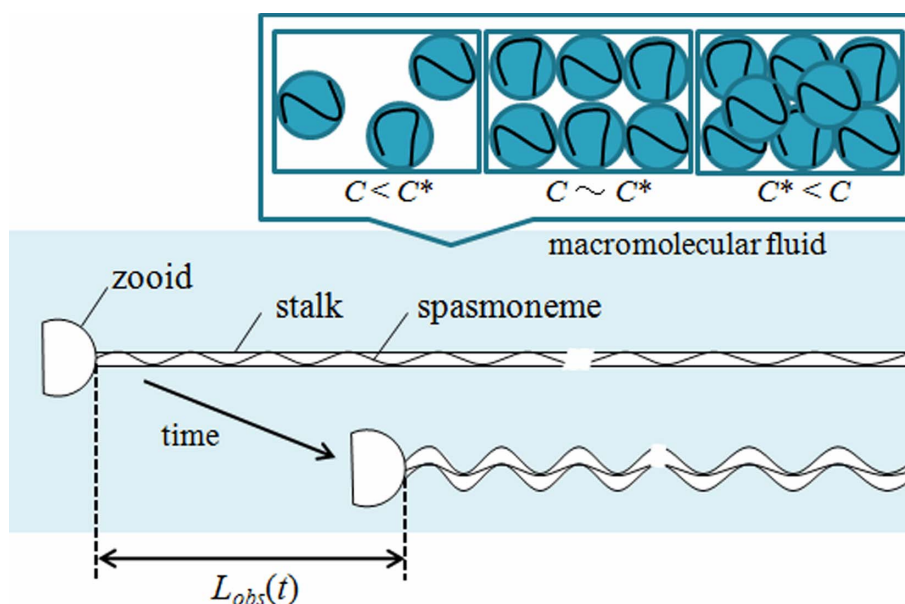
Figure 1 Schematic image of the contraction of *Vorticella* sp. in a macromolecular environment.

mentally different from many other types of biological movements such as the contraction of muscles and ciliary motility[10].

The contraction process of living *Vorticella* sp. has been studied by a few researchers[7–11]. The motion of a zooid has been considered to be similar to the behavior of a damped harmonic oscillator; in this case, the stalk of the zooid is subjected to a Hookean spring force and the zooid is subjected to a frictional force. The solution of the equation for the overdamped system is a double exponential function. However, a single exponential instead of a double exponential function was applied to the experimental data for the latter stage of the contraction process[8,9]. In the previous paper, we attempted to fit the entire contraction process of living *Vorticella* sp. using a double exponential function and a stretched exponential function[11]. A stretched exponential is more suitable for explaining the contraction process than a double exponential function. The stretched exponential function is deduced from the model in which the spasmoneme consists of small segments and the segments contract through nucleation and growth. This implies that the nucleation starts near the zooid and spreads downwards along the spasmoneme in a one-dimensional space. This model can describe the practically observed contractile process in which the contraction of the stalk begins near the cell body and spreads downwards along the spasmoneme.

The motion of microorganisms has been known to be affected by the external fluid viscosity[9,12–14]. For example, Berg and Turner reported that the rotation rate of *Escherichia coli* ($0.5 \times 10 \, \mu$m) is decreased by adding a polymer to the culture media. The swimming speed of *Escherichia coli* in hydroxypropyl methylcellulose is greater than that in Ficoll at the same viscosity. The dependence of the rotation rate on the viscosity of the polymer solution is expressed by a power law with an index value of 0.5 for hydroxypropyl methylcellulose and 1.0 for Ficoll. The contraction speed of living *Vorticella convallaria* in a macromolecular environment has been investigated by Upadhyaya et al.[9]. The viscosity of the external fluid was varied by adding polyvinyl pyrrolidone ($M_w = 360,000$); the viscosity was adjusted from 1 to 5 mPa·s. The dependence of the maximum speed on the viscosity was described by a power law with an index value of 0.5. In this report, the viscosity effect on the contraction process of living *Vorticella* sp. has been investigated using several types of polymer additives such as hydroxypropyl cellulose, polyethylene oxide, and Ficoll for viscosities ranging from 1 to 5 mPa·s, and the investigation is on the basis of both the nucleation and growth model and the overdamped spring model.

In order to characterize the additive polymer and to understand the state of the polymer solution, we refer to the critical overlap concentration (C^*) of the polymer solution, as shown in Figure 1. The polymer molecules are isolated from each other in the dilute regime and they begin to be entangled with each other at concentrations higher than C^*. Three types of critical overlap concentrations, C_s^*, C_v^*, and C_r^*, have been used in this study. C_s^* is evaluated as $C_s^* = 3M_w/4\pi R_g^3 N_A$, where M_w, R_g, and N_A are the weight-average molecular weight, the radius of gyration, and the Avogadro number, respectively[15,16]. C_v^* is calculated by $1/[\eta]$, where the intrinsic viscosity $[\eta]$ is the volume occupied by a polymer per unit mass and deduced from $[\eta] = \lim_{C \to 0}(\eta_{sp}/C)$[17,18]. η_{sp} is defined as $\eta_{sp} = (\eta - \eta_0)/\eta_0$, where η and η_0 are the viscosities of the aqueous solutions of the polymer and water, respectively. C_r^* is deduced from the double logarithmic plot of η_{sp} vs. $C[\eta]$[15,19,20]. η_{sp} increases approximately linearly

with an increase in the polymer concentration C, but the slope changes abruptly at high values. The plots have been characterized by the existence of two different slopes that intersect for a given value of $C[\eta]$, which enables the determination of the rheological overlap concentration, C_r^*. In this study, the limit between the different concentration domains is shown to be characterized by C_r^* and the static overlap concentrations, C_s^* and C_v^*; dilute solutions are those for which for $C < (C_s^*, C_v^*)$ and semi-dilute solutions are the ones for which $(C_s^*, C_v^*) < C < C_r^*$.

Experiments

Vorticella sp. in vivo was obtained from activated sludge. The exact procedure is described in our previous paper[11]. An aqueous solution of KCl (0.10 M), $CaCl_2 \cdot 2H_2O$ (0.09 M), and $MgSO_4 \cdot 7H_2O$ (0.01 M) was used as a culture medium. Hydroxypropyl cellulose (HPC; M_w=30,000–1,000,000), polyethylene oxide (PEO20K; M_w=20,000, PEO500K; M_w=500,000), and Ficoll (M_w=4,000,000) were purchased from Wako Pure Chemical Industries, Ltd. as viscosity modifying agents. The viscosities of the aqueous solution media of these polymers with various concentrations were measured at 25°C using a vibrational viscometer (VM-100; Sekonic Co.).

The contraction processes of two *Vorticella* sp. single cells attached to glass rods were observed; hydroxypropyl cellulose or Ficoll was used as the polymer additive in the medium for one cell and PEO20K or PEO500K was used for the other. In order to initiate contraction, the cell was stimulated by hitting the dish. The contraction process was observed using an inverted microscope (IX70; Olympus Co.) after immersing the cell in the objective medium for 15 min at 21°C, as shown in Figure 2. The bright field microscope images were recorded using a high-speed video camera system (Ektapro High Gain Imager and Hi-spec Motion Analyzer; Eastman Kodak Co.) at a speed of 4000 frames/s. The measurements were performed two times under the same conditions. Before replacing the external fluid by another fluid with a different type of polymer or a different polymer concentration, the cell was kept in the culture media without any polymer additive for more than 3 h or 3 min, respectively.

The microscope images were transferred to a personal computer using a video board (Power Capture Pro; Canopus) and processed with Adobe Premiere 6.0 (Adobe Systems Inc.) at a spatial resolution of 640×480 pixels (1 pixel $=1.3 \times 10^{-3}$ mm). The programs for graphical analysis and curve fitting were developed using Delphi 3.1 (Borland Co., Ltd.). Various fitting functions can be estimated for all data curves by the nonlinear least-squares method based on the quasi-Marquardt algorithm using PLASMA software[23,24]. Calculations were carried out on a personal computer (SF SV2408/B4; Microsoft Windows 2000).
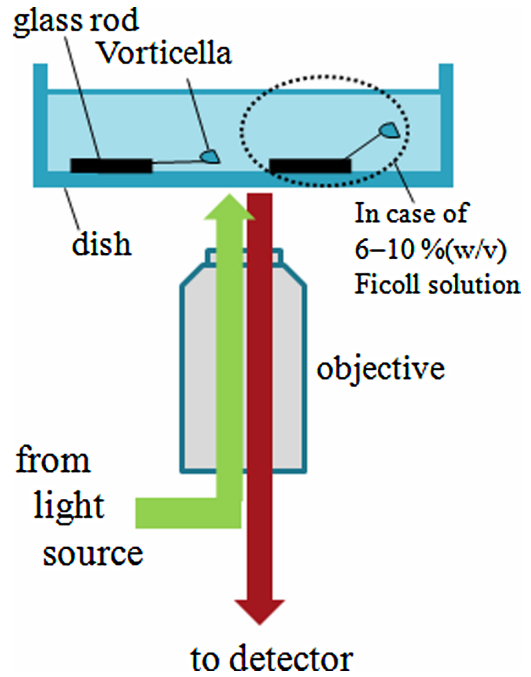

Figure 2   Schematic diagram of the experimental setup.

Results and Discussion

A schematic image of the contraction of *Vorticella* sp. in a macromolecular environment is shown in Figure 1. In *Vorticella* sp., a bell-shaped zooid is attached to a substrate through a slender stalk. The stalk is straight at the initial stage. Then, it bends and coils into a helix near the zooid. Subsequently, the contraction spreads to the base of the stalk. The coordinates of the junction between the zooid and the stalk were tracked in order to determine the reduced length resulting from the contraction of the stalk; the length of the fully contracted stalk is assumed to be zero. Figure 3 shows the temporal changes in the reduced length, $L_{obs}(t)$, for *Vorticella* sp. in various aqueous culture media with polymer additives, i.e., HPC, PEO500K, PEO20K, and Ficoll. The viscosities of the external fluids were modified by adding polymers to the culture media. The concentrations of polymer additives, denoted by C, are 0–0.3% (w/v) for HPC, 0–0.5% (w/v) for PEO500K, 0–5% (w/v) for PEO20K, and 0–10% (w/v) for Ficoll. These polymer additives provide viscosities ranging from 1 to 5 mPa·s. The critical overlap concentrations C_v^* (=1/$[\eta]$) for various polymer additives are listed in Table 1, where $[\eta]$ is determined by the extrapolation of η_{sp} to zero polymer concentration, as shown in Supplementary Figure S1. Each value of C_v^* is lower than the maximum concentration of HPC, PEO, and Ficoll. On the other hand, the rheological critical overlap concentration, C_r^*, is considered to be higher than the maximum concentration because only one slope exists in the double logarithmic plot of η_{sp} vs. $C[\eta]$, as shown in Figure 4. The reference data about C_s^*, C_v^*, and C_r^* are also listed in Table 1 and
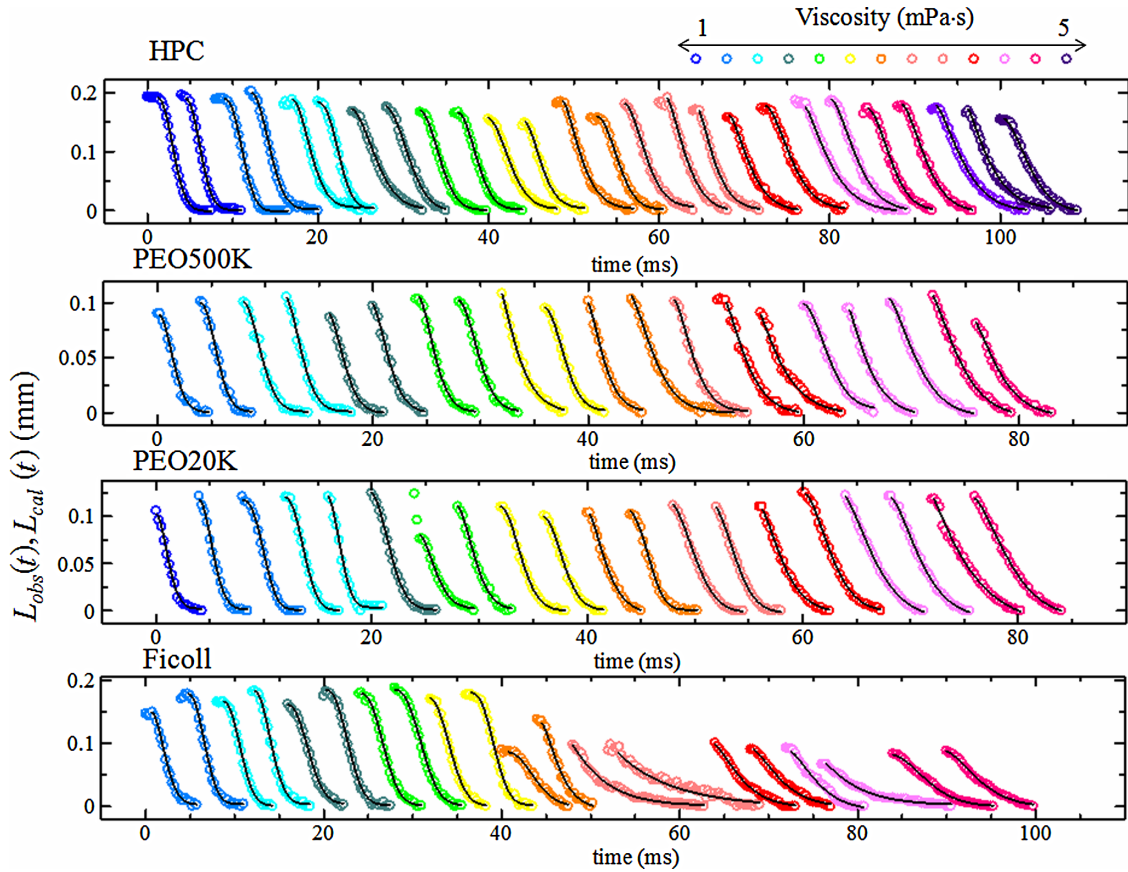
Figure 3 Temporal change in the reduced length, $L_{obs}(t)$, resulting from the contraction of the stalk in aqueous culture media of HPC, PEO500K, PEO20K, and Ficoll with various concentrations for viscosities ranging from 1 to 5 mPa·s. $L_{obs}(t)$ is displaced as the starting time of the contraction increases with an increase in viscosity. The solid line is a stretched exponential function (Eq. (2)) with arbitrary t_0.

Table 1 Characteristics of polymers used in this study, along with reference data

Polymer	Experimental Data				Reference Data					
	M_w	C	$[\eta]^{(a)}$	C_v^*	M_w	R_g (nm)	C_s^*	C_v^*	C_r^*	Ref.
Hydroxypropyl cellulose	30–1000 K	0–0.3	6.744	0.148					$0.445^{(b)}$	
					125 K	31	0.167			21
					150 K	19.8	0.769	0.719	2.16	19
					1000 K	57.3	0.212	0.198	0.594	19
Polyethyleneoxide	20 K	0–5.0	0.353	2.833	22 K			2.53		22
					100 K				11.760	20
					173 K	22.1	0.640	0.680		22
	500 K	0–0.5	4.066	0.246	400 K				2.94	20
					538 K	41.4	0.303	0.278		22
Ficoll	428 K	0–10	0.137	7.299	428 K	20	2.1	6.7		18

The critical overlap concentration C^* % (w/v) is calculated as C_s^* ($=3M_w/4\pi R_g^3 N_A$,), C_v^* ($=1/[\eta]$), and C_r^*.
(a) $[\eta]$ is determined by the extrapolation of η_{sp} to zero polymer concentration, as shown in Supplementary Figure S1.
(b) The value of C_r^* was calculated by substituting the experimental value of $[\eta]$ ($=6.744$) for $C_r^* [\eta]=3$, which holds for various molecular weights in Ref. 19.

these data support the assumption that the rheological overlap concentration C_r^* is higher than the maximum concentration and that the static overlap concentrations, C_s^* and C_v^*, are lower than the maximum concentration. We may consider the external fluids used in this study to be dilute or semi-dilute solutions of polymers, in which the effects of dynamic entanglement induced by the intermolecular interactions of the overlapping chains are not yet observed. Despite the addition of several salts to the external fluid, these effects are not observed because the size of HPC and
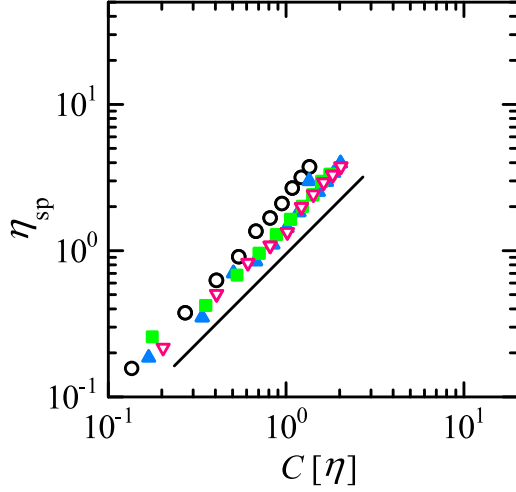
Figure 4 Plots of η_{sp} as a function of $C[\eta]$ for the aqueous solutions of HPC (filled triangle), PEO500K (inverted open triangle), PEO20K (filled square), and Ficoll (open circle).

PEO in aqueous solution has been reported to decrease upon the addition of KCl and CaCl$_2$[25,26]. The value of C^* for HPC, PEO, and Ficoll is expected to increase upon the addition of these salts.

Fitting Functions for the Contraction Process of *Vorticella* sp. in Aqueous Media with Polymer Additives

The following two fitting functions were applied to express the temporal change in the reduced length, $L_{obs}(t)$, owing to the contraction of *Vorticella* sp. A double exponential function is deduced from the damped spring model as follows.

$$L_{cal}(t) = a\exp\left(-(p/2+\sqrt{p^2/4-q})(t-t_0)\right)$$
$$+ b\exp\left(-(p/2-\sqrt{p^2/4-q})(t-t_0)\right),$$
$$p = \frac{6\pi\eta r}{m}, \quad q = \frac{k}{m}, \quad \frac{p^2}{4}-q > 0. \quad (1)$$

where m is the mass of the zooid, r is the radius of the zooid, η is the viscosity of the external fluid, k is the Hookean force constant of the spring, and t_0 is the initial time delay. On the other hand, a stretched exponential function is deduced from the model in which the spasmoneme consists of small segments and the segments contract through nucleation and growth

$$L_{cal}(t) = c\exp\left(-\left(\frac{t-t_0'}{\tau_s}\right)^\beta\right), \quad \beta = \alpha+1. \quad (2)$$

where c is the entire reduced length of *Vorticella* sp., τ_S is the characteristic time of the contraction, α is the space dimension for the contractile process through nucleation for $0\leq\alpha\leq1$, and t_0' is the initial time delay. The goodness of the
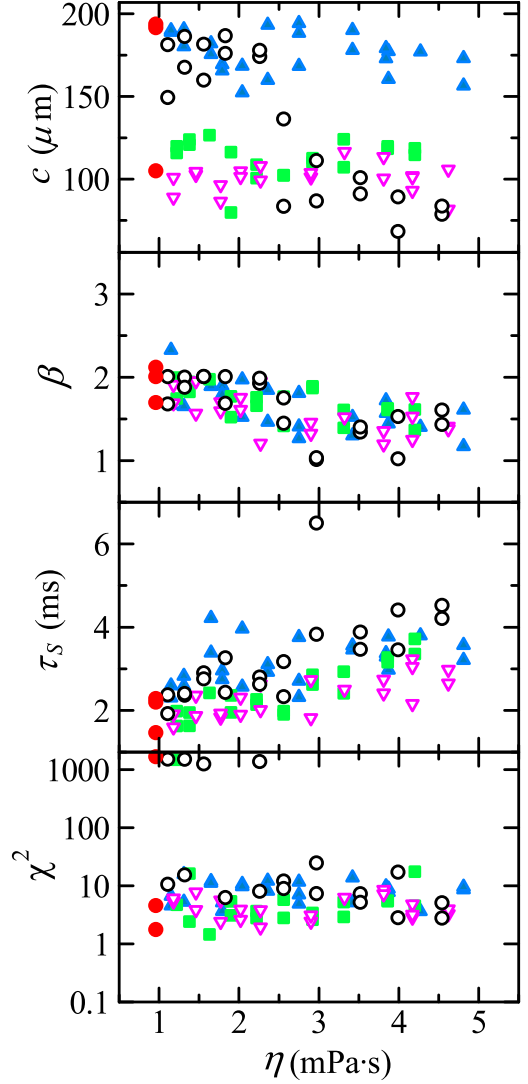

Figure 5 Plots of fitting parameters of Eq. (2) against η for a solution with no polymer additive (filled circle) and the aqueous solutions of HPC (filled triangle), PEO500K (inverted open triangle), PEO20K (filled square), and Ficoll (open circle).

fitting calculation was evaluated by the value of the residual sum of squares, χ^2, as

$$\chi^2 = \frac{1}{t_2-t_1-n}\int_{t_1}^{t_2}(L_{obs}(t)-L_{cal}(t))^2 dt, \quad (3)$$

where n, t_1, and t_2 indicate the number of variable parameters of the fitting function $L_{cal}(t)$, the initial and the final times of the fitting range, respectively.

For *Vorticella* sp. in a medium without any polymer additive, the temporal change in the reduced length, $L_{obs}(t)$, was fitted well by both a double exponential function (Eq. (1)) and a stretched exponential one (Eq. (2)). However, for *Vorticella* sp. in macromolecular aqueous media, $L_{obs}(t)$ was not fitted well by Eq. (1), whereas it was fitted well by Eq. (2), as shown in Figure 3. An example of the fitting of $L_{obs}(t)$

by both Eq. (1) and (2) is shown in Supplementary Figure S2.

The fitting parameters and the residual sum of squares, χ^2, of Eq. (2) are plotted against the viscosity of the external fluid, η, as shown in Figure 5. The fitting values for the case in which no polymer additive is used are also plotted at the lowest η value. The index value of β decreases from 2 to 1 with an increase in η. The fact that the value of β ranges from 1 to 2 is consistent with the model expressed by Eq. (2), in which the contraction occurs through a process similar to nucleation and growth in the one-dimensional space. The space dimension for nucleation, α is obtained by subtracting one from the β value. The fact that the value of β decreases with an increase in the viscosity indicates that the space dimension for the contractile propagation of certain stimuli decreases and the accompanying contractile speed also decreases with an increase in η. The characteristic time of the contraction, τ_S, increases with an increase in η. This result indicates that the contraction becomes slower with an increase in the viscosity of the external fluid upon the addition of polymers. The entire reduced length of *Vorticella* sp., c, is almost constant in HPC and PEO solutions. However, the value of c is low in Ficoll for a viscosity higher than 2.5 mPa·s (6% (w/v)). The stalk appears to be completely extended in the initial stage of the contraction process, which is because of the upward motion of the zooid, which is in turn attributed to the high density of the external fluid. In fact, the density of the Ficoll solution exceeds 1.01_5 g/ml for concentrations higher than 6% (w/v), whereas the densities of HPC and PEO solutions are lower than 1.00_5 g/ml even at 5% (w/v) PEO20K, as shown in Figure 6. We did not observe any deformation of the zooid. Additionally, we supposed that there was no biological insufficiency due to osmosis. The projected length of the stalk appears to be shorter than the actual length when the zooid rises, as shown in Figure 2.

Dependence of Contraction Speed on the Viscosity of the External Fluid with Polymer Additive

The maximum speed of the contraction process, u_{max}, is analytically calculated using Eq. (2) as

$$u_{max} = c\frac{\beta}{\tau_s}\left(1 - \frac{1}{\beta}\right)^{1-\frac{1}{\beta}}\exp\left(\frac{1}{\beta} - 1\right). \tag{4}$$

The evaluated u_{max} for *Vorticella* sp. in aqueous media with polymer additives at various concentrations are plotted as a function of the external fluid viscosity η, as shown in Figure 7. The value of u_{max} monotonically decreases with an increase in η. In the case of Ficoll, the contraction speed is considerably low at concentrations higher than 6% (w/v), where the zooid of *Vorticella* rises owing to the high density of the external fluid. The projected length of the stalk must be shorter than the actual length, especially for 6–10% (w/v) Ficoll solutions. Therefore, the average value of c for *Vorticella* sp. in all the solutions except 6–10% (w/v) Ficoll
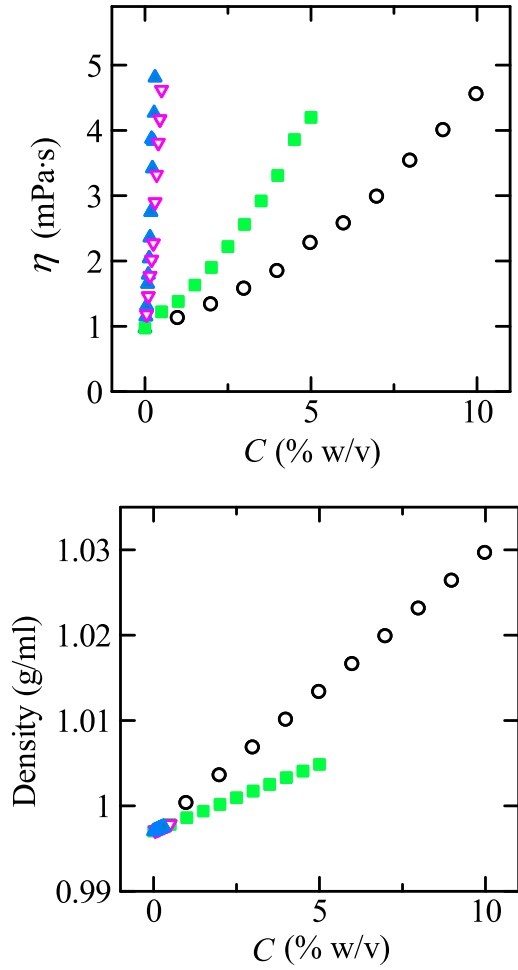

Figure 6 Plots of η and density as a function of the concentration of polymer, C, for the aqueous solutions of HPC (filled triangle), PEO500K (inverted open triangle), PEO20K (filled square), and Ficoll (open circle).

solutions is used to re-evaluate u_{max} using Eq. (4), and the recalculated values of u_{max} are denoted as diagonal cross symbols in Figure 7. The plot of u_{max} against η is described by power law behavior with $u_{max} \sim \eta^s$, where the values of S are -0.3_5, -0.4, -0.5, and -0.5 for HPC, PEO500K, PEO20K, and Ficoll, respectively. Considering that the shear stress for a Newtonian fluid is proportional to the shear rate, the contractile force exerted by *Vorticella* sp. is expressed by $F \sim \eta u$, where F is the contractile force and u is the contraction speed. If the contractile force exerted by *Vorticella* sp., F, is constant, then the contraction speed scales inversely with the viscosity of the external fluid, as expressed by $u \sim \eta^{-1}$. Even for the conventional damped spring model combined with Stokes' law, expressed as $F = 6\pi\eta r u$, u_{max} is calculated using Eq. (1) as

$$u_{max} = 2\sqrt{-ab}\sqrt{p^2/4 - q}\left\{\sqrt{-a/b}\left|\frac{\sqrt{p^2/4-q}+p/2}{\sqrt{p^2/4-q}-p/2}\right|\right\}^{-\frac{p}{2\sqrt{p^2/4-q}}},$$
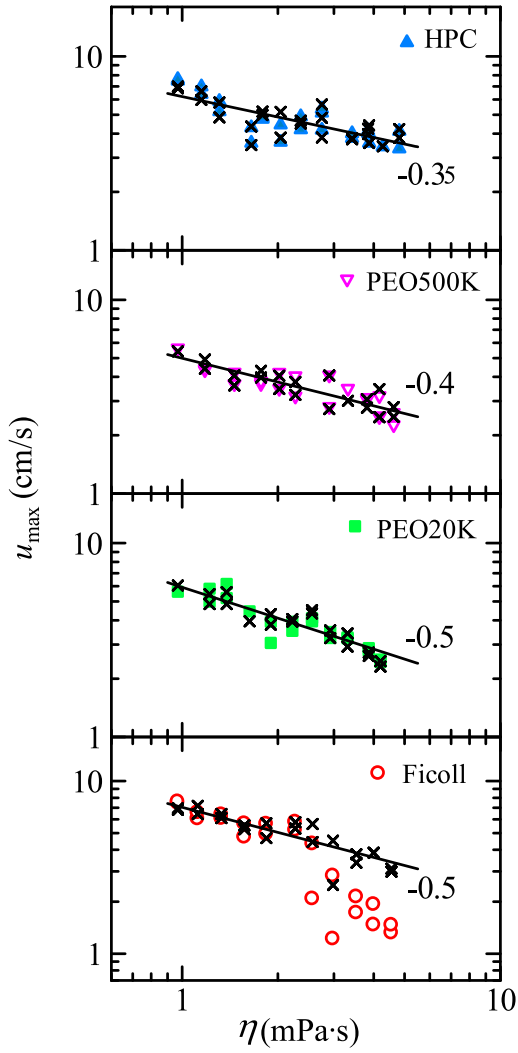
$$\tag{5}$$

Figure 7 Log-log plots of u_{max} as a function of η for the aqueous solutions of HPC (filled triangle), PEO500K (inverted open triangle), PEO20K (filled square), and Ficoll (open circle). The values of u_{max} are also recalculated (see text) and plotted as "×" symbols. The slopes of the lines that fit these values (solid lines) are -0.3_5, -0.4, -0.5, and -0.5 for HPC, PEO500K, PEO20K, and Ficoll, respectively.

and the power law behavior is approximated by $u_{max} \sim \eta^{-1}$, as shown in Supplementary Figure S3. This index value of -1 is lower than those for polymers, where the index values range from -0.3_5 to -0.5. Upadhyaya et al. reported an index value of -0.5 for living *Vorticella convallaria* in polyvinyl pyrrolidone ($M_w = 360,000$) solution with various concentrations; the viscosities in their study ranged from 1 to 5 mPa·s[9]. The decrease in the contraction speed of *Vorticella* sp. in a macromolecular environment is lower than that expected on the basis of Stokes' law. On the other hand, the viscous energy dissipated by the contraction of *Vorticella* sp. is expressed by $P \sim \eta u^2$, where P is the dissipated energy, η is the viscosity of the external fluid, and u is the contraction speed. Assuming that the viscous energy loss P is constant in the contraction process of *Vorticella* sp., the

contraction speed u is related to the external fluid viscosity η as $u \sim \eta^{-0.5}$. This relationship has already been proposed by A. Upadhyaya et al. Although the index value ranges from -0.3_5 to -0.5 in this study, the contraction speed in a macromolecular environment can be roughly expressed by the viscosity of the external fluid as $u \sim \eta^{-0.5}$, for viscosities ranging from 1 to 5 mPa·s.

Upon closer investigation of the index value, the contraction of *Vorticella* sp. may be characterized for each polymer as follows. The plot of u_{max} against η is represented by $u_{max} \sim \eta^s$, where the values of S are -0.3_5, -0.4, -0.5, and -0.5 for HPC, PEO500K, PEO20K, and Ficoll, respectively. These values indicate that when the viscosity of the external fluid is constant, u_{max} decreases in the following order —HPC $\approx$ PEO500K, PEO20K $\approx$ Ficoll. Ficoll is a highly branched polymer with a roughly spherical shape, whereas HPC and PEO are linear polymers. The contraction behavior of *Vorticella* sp. does not seem to be as significantly affected in the linear polymer solution as in the globular polymer solution. The apparent viscosity is introduced for the contraction process of *Vorticella* sp.; the apparent viscosity of the linear polymer solution is lower than that of the globular polymer solution. In general, the viscosity of the aqueous solution of a linear polymer is higher than that of a globular polymer solution for the same concentration. This difference in viscosity arises because linear polymer chains hold and drag a relatively large number of water molecules compared to the globular chains. In fact, the critical overlap concentration C_v^* decreases in the following order: Ficoll, PEO20K, PEO500K, and HPC. Linear chains such as HPC and PEO drag a large number of solvents and consequently increase the viscosity of their solution η; however, the increase in the apparent viscosity for the zooid of *Vorticella* sp. is not as high as the increase in η. This polymer effect might be related to the shear-thinning behavior at high shear rates[19,27] or to the concept of "microscopic viscosity (microviscosity)" for a system in which a continuous and homogeneous solvent does not hold[28,29]. The shear rate of the medium water flow around *Vorticella* sp. is estimated to be 1.7×10^4 [1/s] using the parameters of the damped spring model—the generated force of 4.58×10^{-8} N in the initial stage of the contraction, the viscosity of water, i.e., 1.0 mPa·s, and the zooid radius of 30 μm[11]. The shear rate of *Vorticella* sp. seems to be considerably high, and this may cause the shear-thinning behavior through the disentanglement of the polymer coils in solution and the increased orientation of the polymer coils in the direction of the flow. The flow encounters decreased resistance at higher shear rates and the apparent viscosity is lower, especially for linear polymer chains such as HPC and PEO. On the other hand, experiments on the diffusion of solvents with viscose cosolvents showed that the solvent viscosity in the microenvironment, η^{**}, (microviscosity), is represented in terms of the bulk viscosity η^* (macroviscosity) as $\eta^{**} \sim \eta^{*\gamma}$, with $\gamma (0 \le \gamma \le 1) \sim (M_0/M)^{1/3}$, where M_0 and M are the molecular weights of the

solvent and cosolvent, respectively[29]. According to this equation, the microviscosity of the PEO500K solution is lower than that of the PEO20K solution. This result is consistent with the fact that the contractile speed of *Vorticella* sp. is higher in PEO500K than in PEO20K for the same external viscosity (macroviscosity).

Conclusion

The contraction process of living *Vorticella* sp. in a macromolecular environment with various viscosities has been investigated by image processing using a high-speed video camera. The viscosity of the external fluid ranges from 1 to 5 mPa·s for different polymer additives such as Ficoll, PEO20K, PEO500K, and HPC. The contraction processes are fitted well by a stretched exponential function rather than a double exponential function. The stretched exponential function is deduced from the nucleation and growth model and explains the practical process in which the contraction of the stalk starts near the zooid and spreads downwards along the stalk. The experimentally evaluated index values of the stretched exponential range from 1 to 2 and are consistent with the model in which the contraction occurs in the one-dimensional space.

The maximum speed of the contraction decreases monotonically with an increase in the external viscosity, in accordance with power law behavior. The index value is -0.3_5, -0.4, -0.5, and -0.5 for HPC, PEO500K, PEO20K, and Ficoll, respectively. If the viscous energy dissipated by the movement of the zooid is constant, then the contraction speed of *Vorticella* sp. in a macromolecular environment can be roughly expressed by the viscosity of the external fluid as $u \sim \eta^{-0.5}$. Upon closer investigation of the index value, we can infer that when the viscosity of the external fluid is constant, the contraction speed decreases in the following order—HPC ≈ PEO500K, PEO20K ≈ Ficoll. This polymer effect might be attributed to the shear-thinning behavior at high shear rates or to the concept of "microviscosity" for the system in which a continuous and homogeneous solvent does not hold.

References

1. Huck, W. T. S. Responsive polymers for nanoscale actuation. *Materials today* **11**, 24–32 (2008).
2. Hoffmann-Berling, H. Der mechanismus eines neuen, von der muskelkontraktion verschiedenen kontraktionszyklus. *Biochim. Biophys. Acta* **27**, 247–255 (1958).
3. Weis-Fogh, T. & Amos, W. B. Evidence for a new mechanism of cell motility. *Nature* **236**, 301–304 (1972).
4. Amos, W. B. Structure and Coiling of the Stalk in the Peritrich Ciliates Vorticella and Carchesium. *J. Cell Sci.* **10**, 95–122 (1972).
5. Asai, H. Ca²⁺-driven contraction of spasmoneme in *Vorticellidae*. *Jpn. J. Protozool.* **38**, 133–152 (2005).
6. Katoh, K. & Naitoh, Y. Control of cellular contraction by calcium in *Vorticella*. *J. Exp. Biol.* **189**, 163–177 (1994).
7. Jones, A. R., Jahn, T. L. & Fonseca, J. R. Contraction of protoplasm. IV. Cinematographic analysis of the contraction of some peritrichs. *J. Cell. Physiol.* **75**, 9–19 (1970).
8. Moriyama, Y., Hiyama, S. & Asai, H. High-Speed Video Cinematographic Demonstration of Stalk and Zooid Contraction of Vorticella convallaria. *Biophys. J.* **74**, 487–491 (1998).
9. Upadhyaya, A., Baraban, M., Wong, J., Matsudaira, P., van Oudenaarden, A. & Mahadevan, L. Power-Limited Contraction Dynamics of Vorticella convallaria: An Ultrafast Biological Spring. *Biophys. J.* **94**, 265–272 (2008).
10. Misra, G., Dickinson, R. B. & Ladd, A. J. C. Mechanics of Vorticella Contraction. *Biophys. J.* **98**, 2923–2932 (2010).
11. Kamiguri, J., Tsuchiya, N., Hidema, R., Yatabe, Z., Shoji, M., Hashimoto, C., Pansu, R. B. & Ushiki, H. Contraction Behaviors of *Vorticella* sp. Stalk Investigated using High-Speed Video Camera. I: Nucleation and Growth Model. *Biophysics* **8**, 1–9 (2012).
12. Schneider, W. R. & Doetsch, R. N. Effect of viscosity on bacterial motility. *J. Bacteriol.* **117**, 696–701 (1974).
13. Berg, H. C. & Turner, L. Movement of microorganisms in viscous environments. *Nature* **278**, 349–351 (1979).
14. Magariyama, Y. & Kudo, S. A Mathematical Explanation of an Increase in Bacterial Swimming Speed with Viscosity in Linear-Polymer Solutions. *Biophys. J.* **83**, 733–739 (2002).
15. Ghzaoui, A. El, Trompette, J. L., Cassanas, G., Bardet, L., Fabregue, E. Comparative Rheological Behavior of Some Cellulosic Ether Derivatives. *Langmuir* **17**, 1453–1456 (2001).
16. Hashimoto, C., Rouch, J., Lachaise, J., Graciaa, A. & Ushiki, H. Complex macromolecular dynamics: I. Estimation technique for time-resolved emission anisotropy ratio of chromophores incorporated into polymer chains. *Eur. Polym. J.* **40**, 1997–2008 (2004).
17. Lapasin, R. & Pricl, S. *Chapter 4: Rheology of industrial polysaccharides: Theory and applications.* (Rheology of polysaccharide system: Blackie Academic and Professional, London, pp. 250, 1995)
18. Cush, R. C. Diffusion of a rodlike virus in complex solutions. A dissertation submitted to Louisiana State University, etd-0409103–165104 (2003).
19. Clasen, C. & Kulicke, W. M. Determination of viscoelastic and rheo-optical material functions of water-soluble cellulose derivatives. *Prog. Polym. Sci.*, **26**, 1839–1919 (2001).
20. Ebagninin, K. W., Benchabane, A. & Bekkour, K. Rheological characterization of poly (ethylene oxide) solutions of different molecular weights. *J. Colloid Interface Sci.*, **336**, 360–367 (2009).
21. Wittgren, B. & Porsch, B. Molar mass distribution of hydroxypropyl cellulose by size exclusion chromatography with dual light scattering and refractometric detection. *Carbohydrate Polymers*, **49**, 457–469 (2002).
22. Kawaguchi, S., Imai, G., Suzuki, J., Miyahara, A., Kitano, T. & Ito, K. Aqueous solution properties of oligo- and poly(ethylene oxide) by static light scattering and intrinsic viscosity. *Polymer* **38**, 2885–2891 (1997).
23. Ushiki, H. Fluorescence Probes in Polymers and Liquid Crystals-Complex Macromolecular Chain Dynamics—Proposal from Far East—. In Applied Fluorescence in Chemistry Biology and Medicine. (Rettig, W., Strehmel, B., Schrader, S. & Seifert, H. eds.) pp. 325–370 (Springer, New York, 1999).
24. Nakagawa, T. & Oyanagi, Y. *Tokyo Daigaku Shuppan-kai* (Tokyo Daigaku Shuppan-kai, Japan, 1982).
25. Nishio, Y., Chiba, R., Miyashita, Y., Oshima, K., Miyajima, T., Kimura, N. & Suzuki, H. Salt addition effects on mesophase structure and optical properties of aqueous hydroxypropyl cellulose solutions. *Polym. J.* **34**, 149–157 (2002).

26. Masuda, Y. & Nakanishi, T. Ion-specific swelling behavior of poly(ethylene oxide) gel and the correlation to the intrinsic viscosity of the polymer in salt solutions. *Coll. Polym. Sci.* **280**, 547–553 (2002).

27. Dunstan, D. E., Hill, E. K., Wei Y. Direct measurement of polymer segment orientation and distortion in shear: semi-dilute solution behavior. *Polymer* **26**, 1261-1266 (2004).

28. Haines B. M., Sokolov, A., Aranson, I. S., Berlyand, L. & Karpeev, D. A. Three-dimensional model for the effective viscosity of bacterial suspensions. *Phys. Rev. E*, **80**, 041922 (2009).

29. Barshtein, G., Almagor, A., Yedgar, S. & Gavish, B. Inhomogeneity of Viscous Aqueous Solutions. *Phys. Rev. E*, **52**, 555–557 (1995).